Pergamon

PII: S0022-3697(97)00188-1

J. Phys. Chem Solids Vol 59, No. 3, pp. 417–423, 1998

Printed in Great Britain
0022-3697/98 $19.00 + 0.00

GEOMETRIC BOUNDARY EFFECTS ON THE ELECTRONIC PROPERTIES OF FINITE CARBON NANOTUBES

H.-Y. ZHU[a], D. J. KLEIN[a,*], T. G. SCHMALZ[a], A. RUBIO[b] and N. H. MARCH[c]

[a]Texas A&M University at Galveston, Galveston, TX 77553-1675, USA
[b]Fisica Teorica, Universidad de Valladolid, Valladolid, Spain
[c]Department of Materials Science & Engineering, University of Liverpool, Liverpool, UK

(*Received* 2 *June* 1997; *accepted* 30 *June* 1997)

Abstract—Quantum finite-size effects in carbon nanotubes are studied as a function of tube length L and of the type of end structure used to terminate the tube. The "end" structures considered are: tori, open tubes terminated with H atoms, and various caps formed from hemispherical pieces of fullerenes. With different geometric boundaries there arise distinct asymptotic band-gap behaviors as a function of L: damped oscillations decaying as $1/L$, monotonic $1/L$ decay, exponentially decaying, and constant. These asymptotic scaling behaviors are categorized and explained in terms of general characteristics of the frontier orbitals. Implications for nanoscale devices are briefly discussed. © 1997 Elsevier Science Ltd. All rights reserved.

1. INTRODUCTION

Since Iijima's [1] first experimental observation of carbon nanotubes, the production of single-walled nanotubes [2], and theoretical work [3] suggesting that some tubes might be electrically conductive, these structures have become of much interest as novel small-band-gap materials. The extended nanotubes can be either semimetallic or small band-gap semiconductors depending on their "helicity" and radius. The recent measurements of electrical transport in individual carbon nanotubes [4], the realization of a field-emission electron source made of aligned nanotubes for flat display applications [5], and also the theoretical proposal of mixing nanotube structures to form tiny electronic switches (heterojunctions) made only of carbon [6] or $B_xC_yN_z$ composites [7] all show the importance of a comprehensive knowledge of the quantum size effects in the electronic properties of nanotubes when used for technological applications.

In a broad context, the reduction of the dimensionality in semiconductor and metallic systems has led to many new and interesting electronic phenomena [8, 9]. In metallic clusters, the quantum confinement effect gives rise to the observation of "magic numbers" in the mass spectra, connected with the filling of electronic shells. Semiconductor quantum dots also offer the possibility of accessing the discrete level spectra that strongly alter their electronic magnetic and transport properties [10]. All these new aspects connected with finite-size effects should play an important role in the properties of finite carbon nanotubes. The effects of the structure of the tube ends and of finite length in nanotubes are still uncharacterized, and their study constitutes the main objective of the present paper. An open question is: do carbon nanotubes show "magic number" behaviors similar to those of metal clusters? Such effects could conceivably be important when using nanotubes for nanoscale electronic and opto-electronic devices where the transport and optical response will be dominated by such quantum size effects.

A rough estimate of the importance of these quantum size effects can be made. With the utilization of the nearest-neighbor tight-binding (nn-TB) model, we estimate the level spacing upon noting that the π-electron energy levels are bounded by $\mp z\beta$ on either side of the Fermi energy ϵ_F, where $z = 3$ is the coordination number and $\beta \approx 2.5$ eV is the nearest-neighbor electron-hopping integral. Thus a mean level spacing can be given as this range of energies divided by the number of atoms in a tube of given radius R and length L: for a tube with $R \approx 5$ Å and $L \approx 1000$ Å, one then has $\Delta\epsilon \approx (6\text{ eV Å}^2)/RL \approx 1.2$ meV. This is a considerable energy for transport and conductivity measurements. Therefore, small nanotubes can exhibit Coulomb blockade effects and oscillations in the conductivity as already manifested in semiconductor quandum dots [8]. The finite-size effects for nanotubes are then of interest, particularly the band-gap and its behavior and the manner of approach toward the infinite tube limit.

1.1. *Tube classification and first computations*

In more detail, the carbon nanotubes are viewed as being composed in the bulk entirely from hexagonal rings of carbons, and in general may be conceived of [10–13]

*Corresponding author.

as graphite strips rolled into tubes. As such the tubes are characterized in terms of two minimal graphite lattice-vector displacements such as to be equivalent on a tube. Here we follow [11], and express such a pair of vectors as integral multiples, t_+ and t_-, of two ring-center to ring-center basis vectors at 120° to one another, and such that $0 \leq t_- \leq t_+ > 0$. The electronic behavior of infinite tubes is straightforward: tubes with $t_+ - t_-$ divisible by 3 have small band-gaps and are likely to be metallic or semimetallic, while all other tubes have substantially larger gaps (when diameters are similar) [10–13].

For real tubes, however, there remains the question of the possible structures of the ends of the tubes, and naturally there remains the related question of the effects of these end structures on the properties of the tubes. Here we address band-gaps (or better HOMO–LUMO gaps, since the structures are to be finite), it being presumed that the structures are neutral, with one nominally π electron per carbon. Of course the curvature of the nanotubes modifies the hybridization (and often diminishes the value for the β integrals), but most of the discussion here is phrased in terms of the simple nn-TB model, the qualitative conclusions reached being in accord with the checks on the results using more sophisticated computations including σ,π mixing, as will be briefly discussed toward the end of this article.

As one step in understanding such finite carbon nanotubes, we have carried out computations on a few hundred structures, first using the simple nn-TB model. The tubes examined have various (t_+,t_-) tube types: first, with the tube diameters $D \approx (0.78\ \text{Å})\{t_+^2 + t_+t_- + t_-^2\}^{1/2}$ being in the range from 5 to 20 Å (and overlapping reasonably with the experimental range ~7–50 Å); and second, with lengths such as to include up to ~500 atoms. The different types of ends or boundary conditions studied include:

- open ends clipped off in different ways with hydrogen atoms taking up the remaining carbon valences at the ends;
- carbon-network caps each corresponding to a half of some fullerene with six pentagons arranged in a physically reasonable pattern satisfying the "isolated-pentagon rule" [14];
- cyclic boundary conditions, whence the tubes may be viewed as forming tori composed solely of hexagons.

Within the TB model a variety of behaviors as a function of tube length L for the HOMO–LUMO gap Δ_L are found depending on the (t_+,t_-) classes and the boundary used to end the tube. The tori within the simple nn-TB model are often exceptional in comparison with the other finite tubes, and will be considered separately. With reference to the infinite (endless) tubes, the asymptotic behaviors can be divided into four classes (with a labelling that will be made clearer in the next section):

Table 1. Variety of band-gap behaviors

Class	t_+,t_- divisible by 3 ($\Delta_\infty^0 = 0$)	t_+,t_- not divisible by 3 ($\Delta_\infty^0 \neq 0$)
d	$\Delta_L \approx A_L/L$	$\Delta_L \approx \Delta_\infty + A/L$
d′	$\Delta_L \approx A/L$	$\Delta_L \approx \Delta_\infty + A/L$
e	$\Delta_L \approx Ae^{-\xi L}$	$\Delta_L \approx \Delta_\infty + Ae^{-\xi L}$, $\Delta_\infty < \Delta_\infty^0$
e′	$\Delta_L = 0$	$\Delta_L = \Delta_\infty < \Delta_\infty^0$

(d) The gap diminishes toward the infinite-tube result with periodic oscillations in L of amplitude quenching as $1/L$.

(d′) The gap diminishes toward the infinite-tube result monotonically as $1/L$.

(e) The gap approaches exponentially fast (with increasing L) a value (usually) different from that for the infinite tube.

(e′) The gap is constant at a value different from that for the infinite tube.

The gap of the infinite tube (with cyclic boundary conditions) is not necessarily that of the finite tubes even as their length becomes ever larger. We subdivide each of these classes into two depending on whether the infinite tube has a zero gap (i.e., when $t_+ - t_-$ is divisible by 3) or a gap unequal to zero (when $t_+ - t_-$ is not divisible by 3). E.g., class (d) divides into (d_0) and $(d_{\neq 0})$.

These various cases are summarized in Table 1. There, Δ_L denotes the gap for a tube of length L, Δ_∞ denotes the limit to which Δ_L approaches, and Δ_∞^0 denotes the gap value for the infinite tube with the usual cyclic boundary conditions. The L-independent parameter A depends on the tube ends, while A_L indicates a parameter which depends periodically on L. The L-independent "scale" parameter ξ depends only on (t_+,t_-). Particular examples for these 0 and $\neq 0$ cases are shown in the gap vs. L plots of Figs 1 and 2. In Fig. 1 cases (d_0) and (e_0) are shown, while case (e_0') is not shown but occurs (e.g.) for the open-ended tube with $(t_+,t_-) = (6,6)$ or $(12,0)$ when the ends are of the form in Fig. 3(c). The only cases found of (d_0') are when $t_- = 0$ and t_+ is divisible by 3, as for $(t_+,t_-) = (9,0)$ with a fullerene cap. In Fig. 2 examples for $(d_{\neq 0}')$, $(e_{\neq 0})$ and $(e_{\neq 0}')$ are shown. Figs 1 and 2 also show gaps for a couple of tori, which will be discussed later. In several cases the behaviors displayed in the figures have been checked to notably longer lengths and have been found to persist, so that the true asymptotic behaviors are presumably revealed even on such relatively short tubes (and such is supported by the arguments of the next section). A few cases, such as $(t_+,t_-) = (5,0)$ with ends as in Fig. 3(d), seem to show a rather slow convergence toward the asymptotic value, although as

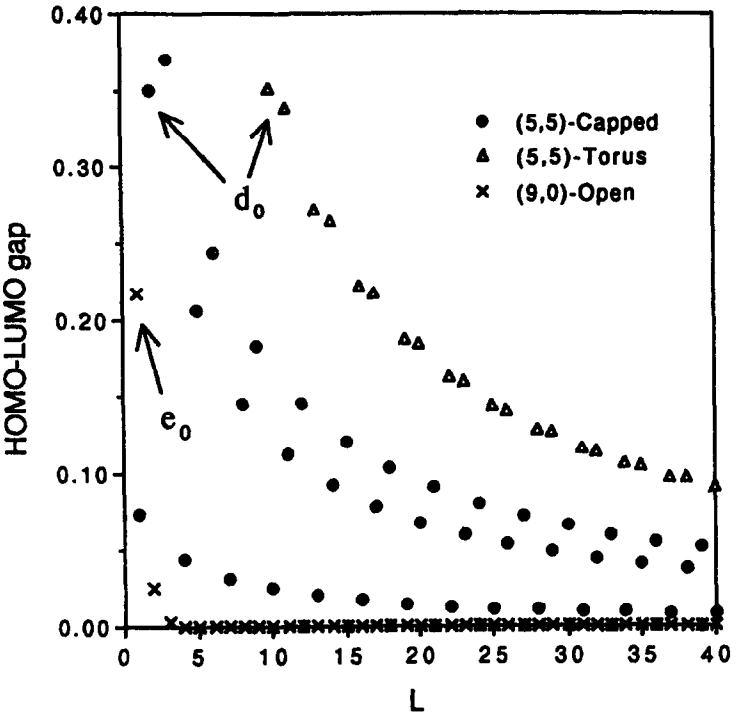

Fig. 1. Gap (in units of β) vs. tube length L (in unit-cell lengths 2.45 Å for (n,n) tubes and 4.26 Å for (n,0) tubes), for different cases where the infinite tube has a zero-gap. There are two cases of (d_0) at $(t_+,t_-) = (5,5)$ and one case of (e_0) at $(t_+,t_-) = (9,0)$; the solid-dot (d_0) case involves a C_{5v} cap which is half of a buckminsterfullerene cage.

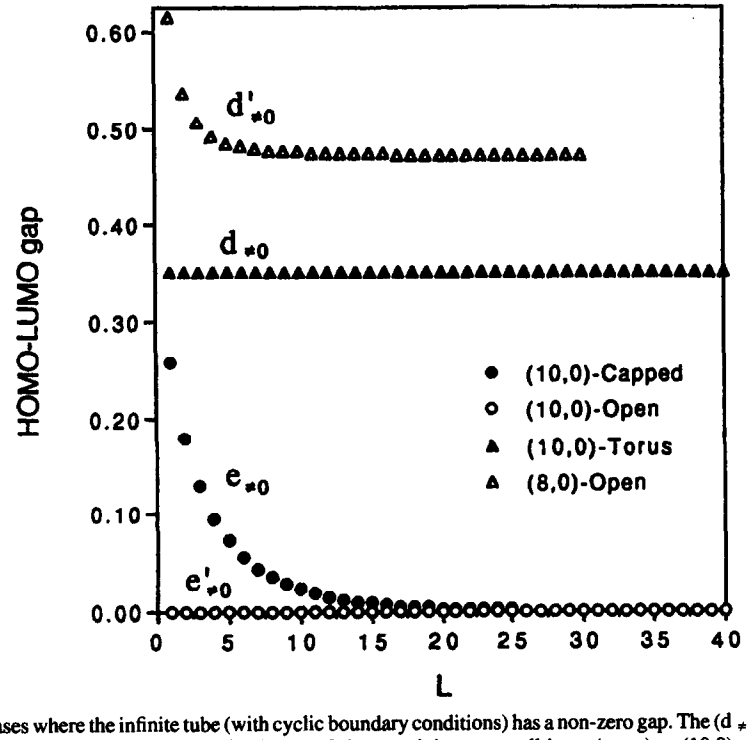

Fig. 2. Gap vs. L for cases where the infinite tube (with cyclic boundary conditions) has a non-zero gap. The ($d_{\neq 0}'$) case is for $(t_+,t_-) = (8,0)$ with open ends of the form indicated in Fig. 3(a), and the remaining cases all have $(t_+,t_-) = (10,0)$: case ($d_{\neq 0}''$) tori, with delocalized frontier orbitals; ($e_{\neq 0}$) tubes with caps as in Fig. 3(d); and ($e_{\neq 0}'$) open-ended tubes as in Fig. 3(c), as well as tubes with C_{5v} symmetry caps from icosahedral C_{80} fullerene.

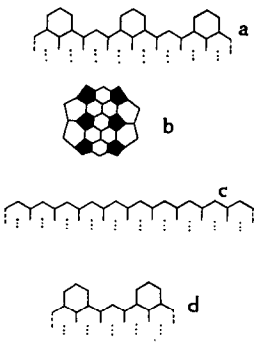

Fig. 3. Different types of tube ends mentioned at different times in the text. In (a), (c), and (d) the dashed bonds at the left and right are the same (the structure being bent into a circle to form a cylinder) and the tube structure continues onward (for a length L) in the downward direction.

we argue in the next section this case should ultimately fall into one of our classes—presumably ($d \neq 0'$).

1.2. *Explanation*

As a first step towards explanation it may be noted that the observed variety of HOMO–LUMO behaviors correlates with the character of the frontier orbitals (i.e., the HOMO and the LUMO). In correspondence to the already noted gap behaviors, there are two broadly different behaviors for the electron density distributions of these frontier orbitals:

> (d & d′) delocalized (or bulk) orbitals (with densities more or less uniform along the length of the tube), the individual orbitals having a helical repetition pattern in case (d) and non-helical in case (d′);
> (e & e′) end-localized orbitals, with in case (e) an inverse localization length ξ such that the density falls like $e^{-\xi x}$ as a function of the distance x to the nearer end and in case (e′) completely end-localized orbitals (for which the density drops to 0 in the bulk of the tube). Frontier orbital densities for examples of such delocalized and end-localized cases are displayed as a function of the tube's axial coordinate in Fig. 4.

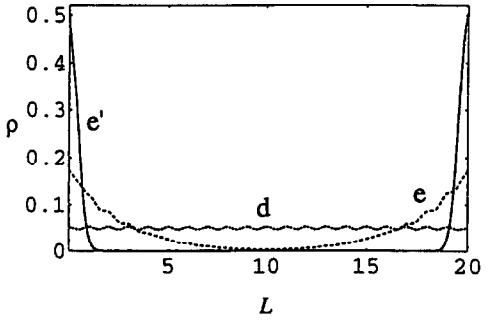

Fig. 4. Density vs. axial position for the frontier orbitals of $(t_+,t_-) = (10,0)$ tubes with length $L = 20$. The type (d) case is for a torus, the type (e) case is for a tube capped as in the inset of Fig. 1(b), with end-localized charge density, and the (e′) case is for an open tube with completely end-localized charge density. These cases are correlated with the different behaviors of the band-gap shown in Fig. 1.

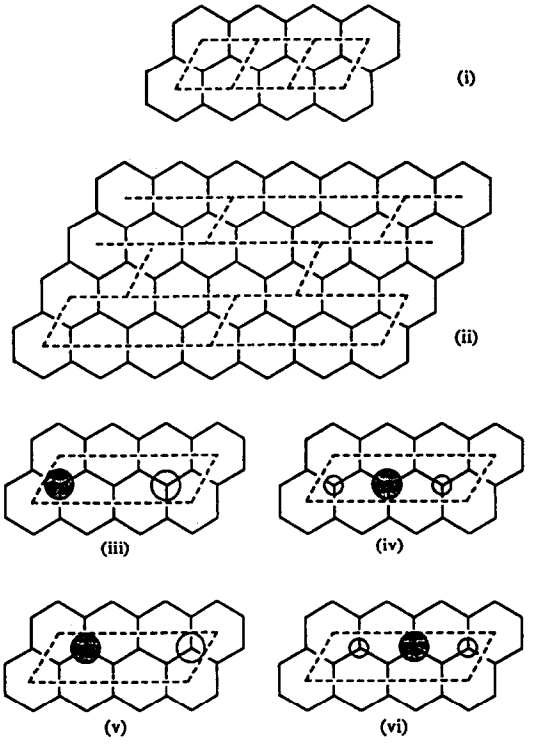

Fig. 5. In (i) the 1×3 super-cell, and in (ii) their manner of inter-relation. In (iii)–(vi) the four associated occupancy patterns for zero-energy orbitals, with open and shaded circles indicating opposite-signed amplitudes; in (iv) and (vi) the smaller circles correspond to half the amplitude of the larger ones.

Evidently a structural characterization of the frontier orbitals is desired, and for the nn-TB model this can be achieved to some degree. For a bipartite system (i.e., with A and B sublattices) it is known [15] that the π-MO energies are symmetrically distributed about the average energy. Thus with

$$H_{nn-TB} \equiv \beta \sum_{i\sim j} \sum_{\sigma} (a_{i\sigma}^{+} a_{j\sigma} + a_{i\sigma}^{+} a_{j\sigma})$$

one has the levels symmetrically arranged around 0, which for the half-filled band case of interest here corresponds to the Fermi energy $\epsilon_F = 0$. Now it is wished to characterize zero-energy MOs, or those (frontier) MOs nearest to 0.

A simple pictorial condition for the existence and character of delocalized zero-energy eigen-orbitals is possible. To this end consider a construction based on a 1×3 super-cell of unit cells cut from the graphite lattice, as indicated in Fig. 5(i), with different such super-cells related as indicated in Fig. 5(ii). The patterns in Fig. 5(iii)–(vi) are to represent possible orbitals with the larger circles indicating amplitudes twice those on the smaller circles and the shading or openness of

the circles indicating the sign of the contribution of the amplitudes. If the whole lattice can be so covered by such super-cells, then with the occupation of every super-cell in one of the four patterns of Fig. 5(iii)–(vi) there results a frontier eigen-orbital ψ_0; that is, if ψ_0 within a super-cell is chosen as indicated in Fig. 5(iii), (iv), (v), or (vi) with all the neighboring cells around it having this same occupation pattern, then (at least within this central super-cell) $H_{nn-TB}\psi_0 = 0$. The result is that zero-gap delocalized orbitals arise for finite structures if and only if the boundary conditions are suitable, both around the tube and at the ends of the tube. Thus, if the infinite tube or a torus can be (disjointly) covered by such super-cells, then these patterns give zero-gap orbitals. (For the infinite tube this covering condition is just that $t_+ - t_-$ be divisible by 3). For other finite-L tubes associated with an infinite-L tube which can be so covered, the band-gap should fall like $1/L$ toward 0 as L increases—the fraction $\sim 1/L$ arising here because this is the fraction of the super-cell patterns abutting to the ends (where the satisfaction of the zero-eigenvalue condition may fail). A period-3 oscillation in the gap can arise in correspondence with the period-3 manner in which the 1×3 super-cells match to the ends. In this regard $t_- = 0$ plays a special role, as in this case (with t_+ divisible by 3) the long axis direction of the super-cells can follow around a tube circumference, coming back on itself after $t_+/3$ cells. Then the same abutments to the ends occur independently of L and no period-3 oscillation results. But this argument fails for $t_- \neq 0$, since following along the long axis of the super-cells leads from one end of the tube to the other, so that the manner of abutment of the super-cells to the ends oscillates with period 3.

The other zero-gap cases (e_0) and (e_0') with $t_+ - t_-$ divisible by 3 still have bulk orbitals which close in tightly on either side of ϵ_F, but there just happen to be end-localized orbitals at the Fermi level ϵ_F, at least in the $L \to \infty$ limit. This limit is relevant here because these end-localized orbitals typically decay exponentially into the interior of the tube and so interact in pairs (from opposite ends) with a strength $\sim e^{-\xi L}$ and so give a gap $\sim e^{-\xi L}$, as in case (e_0). If it should happen that the end-orbitals are completely localized on the ends (with no gradual decay into the interior), then the case (e_0') of L-independent zero-gap is obtained.

The remaining cases ($d_{\neq 0}$), ($d_{\neq 0}'$), ($e_{\neq 0}$), ($e_{\neq 0}'$) often (but not always) give a gap unequal to zero persistently. The bulk (i.e., delocalized) orbitals nearest in energy to ϵ_F always have a gap unequal to 0, so that the only question is whether any end-localized states end up in this gap. For cases ($d_{\neq 0}$) and ($d_{\neq 0}'$) the relevant orbitals are not end-localized and generally such orbitals will have a fraction $\sim 1/L$ of their density next to the ends, so that a gap $\sim 1/L$ occurs. Of course this gap closes toward 0 as the tube diameter is allowed to become large (i.e., the graphitic limit is approached). For cases ($e_{\neq 0}$) and ($e_{\neq 0}'$) end-localized orbitals lie between the bulk orbitals closest to 0, and the types of behavior discussed in cases (e_0) and (e_0') arise, though the gap need not close to 0.

Further, it should be noted that typically both the HOMO and LUMO fall into the same class (d, d', e, e'). Delocalized orbitals reside primarily on the bulk of the tube which in this bulk is a bipartite lattice where (for the nn-TB model) the pairing theorem [15] implies that their energies are distributed equally above and below ϵ_F. End-localized orbitals generally have energies not so distributed but, for case (e_0) or (e_0'), plus and minus combinations give energies split slightly apart equally above and below ϵ_F. There remains the possibility of the ($e_{\neq 0}$) or ($e_{\neq 0}'$) case which could occur for one of the frontier orbitals, while the other is of type ($d_{\neq 0}$). Having (e_0) or (e_0') at the same time as (d_0) would then only occur with ends of different types.

Finally it is conceivable that there may be some cases with accidently slow convergence. Perhaps this could occur for a circumstance with zero-order non-degenerate delocalized and end-localized orbitals which nevertheless are very close in energy, and so interact at smaller values of L before one ultimately dominates and the correct asymptotic behavior is realized. Such a circumstance appears to occur for $(t_+,t_-) = (5,0)$ with ends as in Fig. 3(d): the frontier orbitals are delocalized with some density on the ends, while energetically adjacent eigen-orbitals are primarily end-localized. The energy gap as a function of L for the computationally realizable L does not clearly exhibit the considered behaviors of Table 1—and indeed the energies do not clearly approach that of the (delocalized) infinite nanotube—all as is consistent with an accidental near degeneracy. That is, if behavior other than that described in Table 1 is found, we believe it is simply because the asymptotic regime has not yet been achieved.

Tori make a special case in that they do not have "ends", so that not only are the frontier orbitals delocalized, but also they have no ends with which to interact. The same arguments apply concerning the covering of the structure with the super-cells of Fig. 5(i) as being needed for a zero-gap. For $t_- = 0$ the ability to cover or not is independent of L, depending solely on whether t_+ is divisible by 3, and thus the gap is a constant independent of L. For $t_+ - t_-$ divisible by 3, certainly every third L leads to a zero gap. For $t_+ - t_-$ not divisible by 3 there is a permanent gap, and different behaviors are expected depending on the location of the gap in k-space of the infinite torus. For the sub-case with $t_- = 0$, the gap is at $k = 0$, which is a point always realized for finite L, so that the gap is constant (as already otherwise argued above). For other sub-cases the $L \to \infty$ gap is at another location k_F in k-space, whence the frontier

orbital bands for $L \rightarrow \infty$ should vary quadratically near k_F, so that as the finite-L discretized selections from k-space close in about the minimum, the $L \rightarrow \infty$ gap should be approached $\sim 1/L^2$.

1.3. *Higher-order computations*

There is evidence that our general conclusions are robust beyond the simple nn-TB model. Most simply, one may extend the π-electron tight-binding model to include next-nearest-neighbor interactions and non-identity overlap, so that the new orbital eigenproblem for the orbital energy ϵ is

$$H_{TB}\psi = \epsilon S\psi$$

where it turns out that H_{TB} and S are expressible in terms of the simple nn-TB model. The restriction of these operators to their representations on the one-electron space might be abbreviated to $\mathbf{H}_{TB}$ and $\mathbf{S}$, and we further abbreviate $\mathbf{A} \equiv \mathbf{H}_{nn\text{-}TB}/\beta$. Then [16] for a network solely of degree 3 sites

$$\mathbf{H}_{TB} = \beta\mathbf{A} + \beta'(\mathbf{A}^2 - 3\mathbf{I}) \quad \mathbf{S} = \mathbf{I} + s\mathbf{A}$$

where β' is the next-nearest-neighbor electron-hopping integral, s is the nearest-neighbor overlap, and $\mathbf{I}$ is the identity matrix. As a consequence:

- the eigenorbitals ψ are the same as those of $\mathbf{H}_{nn\text{-}TB}$;
- the eigenvalues ϵ are given directly in terms of corresponding ones λ of $\mathbf{A}$ (or $\mathbf{H}_{nn\text{-}TB}$), as $\epsilon = \{\beta\lambda + \beta'(\lambda^2 - 3)\}/(1 + s\lambda)$; and
- this mapping is monotonic in the region of the Fermi energy, which still occurs at $\epsilon = 0$.

Thus all the earlier comments regarding the HOMO–LUMO gap and frontier orbitals still apply.

But even a much more elaborate TB model [17] including all valence electrons could be considered, and indeed has been applied for a number of the capped tubes. The results here yield qualitatively the same behaviors (but with splitting smaller by a factor of ~ 2, some of which may be anticipated because of the reduction in β arising from misalignment of π-orbitals on a curved surface, and some of which may be anticipated from the dependence on s in the above formula for ϵ). Though the range of tube lengths with these higher-level computations is less, the scaling behaviors found are in accord with those of the more extensive nn-TB computations model already discussed. We have also performed molecular dynamics computations on several of the tubes to check that relaxation effects are very small on the geometries used in the present studies.

2. DISCUSSION

We have presented a comprehensive identification of the possible behaviors of the gap as a function of tube length, as summarized in Table 1, and we have correlated these behaviors with structural features. Generally, excepting the period-3 oscillations, the gap does not increase as L increases, because the non-bulk interactions repelling the two frontier levels fall off with increasing L. The problem of finite-size quantization effects, rather than being a question of 'magic numbers', is better described as a question of 'magic boundary conditions', as mediated by the networks topology.

For high electrical conductivity, what one needs is a gap equal to 0 (or very small) with delocalized bulk orbitals. Basically this does occur for either of the cases (d_0) or (d_0'), and it necessarily occurs for (e_0) or (e_0'), even though the actual frontier orbitals are end-localized. The delocalized orbitals still tighten down toward ϵ_F as L increases, there just being localized orbitals which tighten down faster. But this does not occur for $(d_{\neq 0})$, $(d_{\neq 0}')$, $(e_{\neq 0})$, or $(e_{\neq 0}')$.

In conclusion, we have elucidated the rich variety of realizable behaviors possible for the HOMO–LUMO gap as a function of L, and have correlated this with the types of frontier orbitals which in turn correlate with the bulk tube structure and the cap (or end) structure. The bulk structure and the special nature of the end boundary conditions are both often relevant for the type of band-gap. The effects predicted in the present studies should be observable in conductivity and transport measurements in single-wall nanotubes and also in doped composite nanotubes [7]. Furthermore, the cap-induced localized states close to the Fermi level make such capped nanotubes ideal candidates for use as tips for scanning microscopy and electron emission materials [5], because of the expected coherent electron emission from such cap states.

Acknowledgements—The Texas authors acknowledge research support from the Welch Foundation of Houston, Texas. A.R. acknowledges financial support from EC-TMR (Grant ERB 4061 PI 95-1048) and from JCL (Grant VA25/95). A.R. thanks Dr. W.A. de Heer and Dr. X. Blase for helpful discussions at the beginning stages of this work.

REFERENCES

1. Iijima, S., *Nature*, 1991, **354**, 56.
2. Iijima, S. and Ichihashi, T., *Nature*, 1993, **363**, 603; Bethune, D.S., Klang, C.H., deVries, M.S., Gorman, G., Savoy, R., Vazquez, J. and Beyers, R., *Nature*, 1993, **363**, 605; Ajayan, P.M., *Cond. Mater. News*, 1995, **3**, 9; and references therein.
3. Mintmire, J.W., Dunlap, B.I. and White, C.T., *Phys. Rev. Lett.*, 1992, **68**, 631.
4. Dai, H., Wong, E.W. and Leiber, C.M., *Science*, 1996, **272**, 523.
5. de Heer, W.A., Chatclain, A. and Ugarte, D., *Science*, 1995, **270**, 1179.
6. Chico, L., Crespi, V.H., Benedict, L.X., Shirley, E.L. and Louie, S.G., *Phys. Rev. Lett.*, 1996, **76**, 971; Charlier, J.C., Ebbesen, T.W. and Lambin, Ph., *Phys. Rev. B*, 1996, **53**, 11108.

7. Blase, X., Charlier, J.C., De Vita, A. and Car, R., *Appl. Phys. Lett.*, 1997, **70**, 197. Composite nanotubes were predicted in: Rubio, A., Corkill, J.L. and Cohen, M.L., *Phys. Rev. B*, 1994, **49**, 5081; Miyamoto, Y., Rubio, A., Louie, S.G. and Cohen, M.L., *Phys. Rev. B*, 1994, **50**, 4976, and synthesized experimentally: Stephan, O., Ajayan, P.M., Collier, C., Redlich, P., Lambert, J.M., Bernier, P. and Lefine, P., *Science*, 1994, **266**, 1683; Chopra, N.G., Leyken, J., Cherrey, K., Crespi, V.H., Cohen, M.L., Louie, S.G. and Zettl, A., *Science*, 1995, **269**, 966; Weng-Sieh, Z., Cherrey, K., Chopra, N.G., Blase, X., Miyamoto, Y., Rubio, A., Cohen, M.L., Louie, S.G., Zettl, A. and Gronsky, R., *Phys. Rev. B*, 1995, **51**, 11229.
8. Smith, C.G., *Rep. Prog. Phys.*, 1996, **59**, 235.
9. de Heer, W.A., *Rev. Mod. Phys.*, 1993, **65**, 611.
10. Hamada, N., Sawada, S. and Oshiyama, A., *Phys. Rev. Lett.*, 1992, **68**, 1579.
11. Klein, D.J., Seitz, W.A. and Schmalz, T.G., *J. Phys. Chem.*, 1993, **97**, 1231.
12. Saito, R., Fujita, M., Dresselhaus, G. and Dresselhaus, M., *Appl. Phys. Lett.*, 1992, **60**, 2204.
13. Dunlap, B.I., *Phys. Rev. B*, 1994, **49**, 5643.
14. Schmalz, T.G., Seitz, W.A., Klein, D.J. and Hite, G.E., *J. Am. Chem. Soc.*, 1988, **110**, 1113.
15. Coulson, C.A. and Rushbrooke, G.S., *Proc. Cambridge Philos. Soc.*, 1940, **36**, 193.
16. Zhu, H., Klein, D.J., Seitz, W.A. and March, N.H., *Inorg. Chem.*, 1995, **34**, 1377.
17. Tang, M.S., Chan, C.T. and Ho, K.M., *Phys. Rev. B*, 1996, **53**, 979.